NMR studies of chemical exchange amongst five conformers of a ten-membered ring compound containing two amide bonds and a disulfide †

Alex D. Bain,* Russell A. Bell, Daniel A. Fletcher, Paul Hazendonk, Rob A. Maharajh, Suzie Rigby and John F. Valliant

Department of Chemistry, McMaster University, 1280 Main Street West, Hamilton, Ontario, Canada L8S 4M1. E-mail: bain@mcmaster.ca.

Received (in Gainesville, FL) 13th January 1999, Accepted 7th May 1999

This paper presents experimental measurements which provide a very detailed picture of the free energy surface of a molecule. The compound, *N*,*N*′-dimethyl-*N*,*N*′-(2,2′-dithiobisacetyl)ethylenediamine (a diamino–disulfide, DADS, chelate), is a symmetrical ten-membered ring compound. Five conformers with significant populations are observed in dimethylformamide solution at 300 K. The ring consists of a pair of methylene groups at the top, each of which is bonded to the nitrogen of an *N*-methylamide linkage. The amides are then connected, through a methylene group, to a disulfide linkage, which forms the bottom of the ring. The conformations can be classified according to the stereochemistry of the amide bond. The lowest energy conformer, C, has one amide in the *Z* geometry and one in the *E* geometry. Conformer B, 0.9 kJ mol^{-1} above C, has both amides *Z*. Two other *Z*,*E* conformations, labelled A and E, lie 3.1 and 3.5 kJ mol^{-1}, respectively, above C. Finally, there is a *Z*,*Z* conformer, labelled D, which is 5.6 kJ mol^{-1} above C. NMR lineshape and selective-inversion measurements have permitted estimates of some of the barriers to interconversion amongst these conformers. The barrier from C to A, which involves an inversion of the disulfide, has a barrier ($\Delta G^{\ddagger}$ at 300 K) of 72 kJ mol^{-1}, and the barrier from C to D (an amide rotation) is 80 kJ mol^{-1}. The barrier from A to B, also an amide rotation, is 78 kJ mol^{-1}. Finally, the barrier to conversion of A to E, which is a ring flip process, is 70 kJ mol^{-1}. Although the disulfide can invert when one amide is *Z* and the other is *E* (this process converts conformer C to A), the barrier to this process when both amides are *Z* is too high to be measured accurately. Selective-inversion NMR experiments allowed extension of the lineshape exchange measurements to lower temperatures, so that the Gibbs' free energies above could be separated into entropy and enthalpy contributions. For the C to A process, $\Delta H^{\ddagger} = 72 \pm 1$ kJ mol^{-1} and $\Delta S^{\ddagger} = 0$ within experimental error. For the C to D process, $\Delta H^{\ddagger} = 86 \pm 1.5$ kJ mol^{-1} and $\Delta S^{\ddagger} = 19 \pm 4$ J K^{-1}. For the A to B process, $\Delta H^{\ddagger} = 84 \pm 1.2$ kJ mol^{-1} and $\Delta S^{\ddagger} = 22 \pm 4$ J K^{-1}. For the A to E process, $\Delta H^{\ddagger} = 74 \pm 1$ kJ mol^{-1} and $\Delta S^{\ddagger} = 11 \pm 3$ J K^{-1}.

Introduction

Energy surfaces are an important tool in chemistry. There is always a global minimum for a set of atoms, but there may be many accessible local minima as well. These local minima are connected by saddle points, which represent the barriers to the change of conformation. The understanding of such barriers is crucial to many fields of chemistry. Particularly in biochemistry, the conformation of a molecule is as important as its composition. Many proteins will retain their function if some amino acids are substituted, but if the three-dimensional structure is changed, activity is completely lost. These changes in conformation usually do not break classical chemical bonds; rather, they involve a complex interaction amongst electronic, electrostatic and steric effects. The more data that we can collect on how these effects balance, the better we can understand molecular conformation.

The compound, *N*,*N*′-dimethyl-*N*,*N*′-(2,2′-dithiobisacetyl)-ethylenediamine (a diamino–disulfide, DADS, chelate)[1] (Fig. 1) provides an excellent test case. It is a ten-membered ring containing two amide bonds and a disulfide bond, and in solution there are five different metastable conformers with significant populations. These arise because there is restricted rotation around both the amide and the disulfide bonds, as well as a ring-flip process. In this paper, the geometry of each of these conformers is assigned, and their relative energies determined.

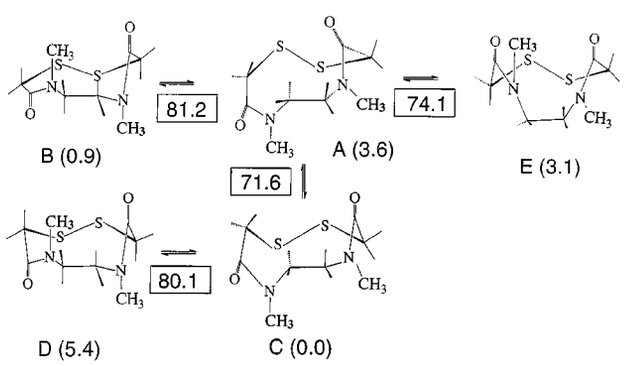

Fig. 1 Structures of the five observable conformers of *N*,*N*′-dimethyl-*N*,*N*′-(2,2′-dithiobisacetyl)ethylenediamine (DADS), labelled A to E. Two are symmetrical (B and D), in which both amides are *Z*, and the others have one amide *Z* and one *E*. The numbers in parentheses are the energies (ΔG^{0} at 300 K) of each conformer above the most stable, C, measured from the NMR spectrum. The numbers in boxes represent the energies ($\Delta G^{\ddagger}$ at 300 K) at the top of each barrier between conformers, again relative to the ground-state energy of C. Each of the barriers can be separated into enthalpy and entropy effects, and can be specified relative to one of the interconverting conformers (see Table 1). Note that the lines without symbols represent bonds to hydrogen, but the symbol H is omitted to simplify the diagram.

† Chemical shifts and coupling constants for the conformers at 273 K and their approximate geometries (Cartesian coordinates in Angstroms) at their local energy minima are available as supplementary data available from BLDSC (SUPPL. NO. 57556, pp. 6) or the RSC Library. See Instructions for Authors available *via* the RSC web page (http://www.rsc.org/authors).

Table 1 Activation parameters for the dynamic processes illustrated in Fig. 1. Since the sites are not equally populated, the values are quoted for the direction indicated. Note that the values in Fig. 1 are all relative to the energy of conformation C, whereas the figures for A-to-B and A-to-C in this table are relative to the energy of conformation A

Process	$\Delta H^{\ddagger}$/kJ mol^{-1}	$\Delta S^{\ddagger}$/J K^{-1}	$\Delta G^{\ddagger}$/kJ mol^{-1} (300 K)
C to A	72 ± 1	3 ± 3	72
C to D	86 ± 1.5	19 ± 4	80
A to B	84 ± 1.2	22 ± 4	78
A to E	74 ± 1	11 ± 3	70

The barriers to four of the exchange processes are reported. A combination of selective-inversion and lineshape NMR experiments over a range of temperatures has permitted the separation of the barrier, $\Delta G^{\ddagger}$, into enthalpy and entropy of activation. The energies of these different conformations, plus the heights of the barriers to interconversion amongst them, give an extraordinarily detailed picture of the potential energy surface of this molecule.

DADS is an important molecule in itself. Certain chelates which contain two nitrogen and two sulfur atoms form stable complexes with ^{99m}Tc, the most widely used agent (at the tracer level) in diagnostic nuclear medicine.[2] The diamino–disulfide (DADS) chelate forms an anionic Tc(v) species which is stable *in vivo*.[3–5] Because of this stability, the DADS-type chelates are popular as a basis for the development of site-specific bifunctional radiopharmaceuticals.[6,7]

Although not a peptide, DADS provides a useful analogy for the study of small, cyclic peptides.[8] The dynamic nature of peptides is well established experimentally, both when only a single, average conformation is observed,[9–12] and when multiple conformers can be seen in an NMR spectrum.[10,13–17] The amide bond[18] and the disulfide[19] both show significant barriers to rotation, and rings define a whole class of dynamic processes. When dynamic effects have been observed in the NMR spectra of peptides, a proline residue is often (but not always[10,15]) involved, since the amide bond in this case is known to adopt both the *cis* and the *trans* conformation.[20] In peptides, a disulfide bond can close a ring, even if two cysteines are next to each other in the sequence.[21,22] Restricted rotation has been observed in both acyclic and cyclic disulfides.[19,23–25] Finally, the exchange among conformations of rings is one of the classic studies in NMR.[26] Cyclohexane[27] is the standard example, and the work continues with recent careful studies of eight-membered[8,28] and ten-membered[29] rings.

Nuclear magnetic resonance (NMR) spectroscopy provides an excellent way of measuring the barriers to all these processes.[26,30] When the exchange rates are comparable to chemical shift differences, characteristic line broadening and coalescence occur in the spectrum. These can be simulated with classic methods,[31,32] or newer approaches[33] in order to estimate the exchange rate. At slower exchange rates, the exchange process competes with spin-lattice relaxation. In this regime, selective-inversion–recovery experiments provide an excellent way of measuring the exchange rate.[34–39] In combination, these methods permit the measurement of rates over a wide range of temperatures,[40] so that the thermodynamics of the transition state can be investigated.

Quoting the Gibbs' free energy of activation, $\Delta G^{\ddagger}$, is equivalent to quoting the rate, since transition state theory says that the rate is given by eqn. (1), in which k is Boltzmann's constant, h is Planck's constant and the transmission factor is unity.

$$\text{rate constant} = \frac{kT}{h}e^{-\Delta G/RT} = \frac{kT}{h}e^{-\Delta H/RT}e^{\Delta S/R} \quad (1)$$

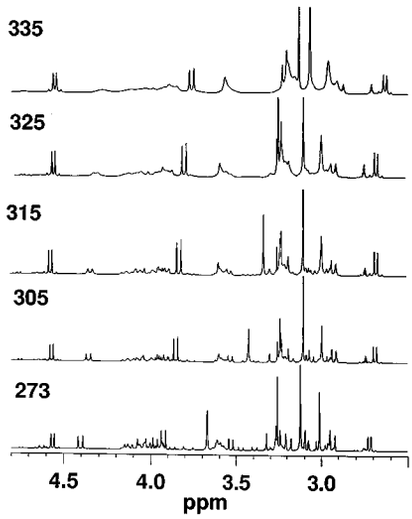

Fig. 2 500 MHz proton NMR spectra of DADS as a function of temperature, in K.

In order to separate the enthalpy and the entropy of activation, the rate constant is measured as a function of temperature, T, and an Eyring plot of log(rate constant/T) *vs.* (1/T) is constructed. This is important, since a measured rate may have a significant entropy contribution, but a calculated potential energy surface[41] involves only enthalpy. It is therefore important to measure the rates over as wide a range of temperatures as possible, to get reliable thermodynamic data.

This work is divided into two parts. The first is qualitative: the assignment of the spectra of each conformation and mapping the mechanism of the exchange. The second is quantitative: measuring the exchange rates as a function of temperature. For the first part, two-dimensional NMR was used extensively, although the precise values of chemical shifts and couplings were determined from a simulation of the equilibrium spectrum. For the quantitative work, one-dimensional experiments were used exclusively. Although two-dimensional experiments can be used quantitatively to extract rate data,[42–44] we believe that one-dimensional experiments are more reliable and more efficient.[34–39,45–48]

Results

The one-dimensional ^{1}H spectra as a function of temperature (Fig. 2) clearly showed that there were multiple conformations exchanging with each other. Quantitative ^{13}C spectra at 253 K identified five species: two of which showed only four carbon peaks, and three species had eight peaks. The first two, conformers B and D in Fig. 1, were assigned to symmetrical conformations in which both amides adopted a Z arrangement.‡ The three non-symmetric species, A, C and E in Fig. 1, had one amide Z and the other E. The relative populations of each species (relative to C, the most populated) are A : B : C : D : E = 0.24 : 0.71 : 1.0 : 0.12 : 0.29. These proportions were measured from Boltzmann population factors in a quantitative ^{13}C NMR spectrum. The proton spectrum of each species was assigned using a two-dimensional Heteronuclear Multiple Bond Correlation (HMBC) experiment (Fig. 3). In this molecule, the amide carbonyl shows long-range coupling to the protons of both the sulfur methylenes and the nitrogen methylenes, so comparison of the carbonyl carbon rows from the HMBC with the proton spectrum (Fig. 4) allowed estimation of the proton chemical shifts. Connectivities of the spectra were confirmed using a gradient COSY (Fig. 5). From these data, a full analysis of each spectrum was performed using the XSIM program (available from Kirk Marat, University of Manitoba). Complete lists

‡ E and Z notation is used for consistency with previous work.[1]

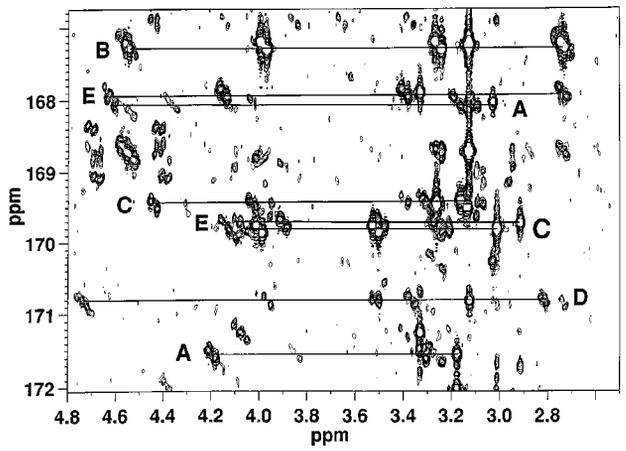

Fig. 3 Contour plot of part of the HMBC spectrum of DADS in dimethylformamide-d_7 at 253 K. The aliphatic region was acquired in the carbon dimension (f_1), but carbonyl signals are folded in and the scale represents the chemical shifts of the carbonyls. The labelled lines highlight the carbonyl signals of each conformation. Of the two closely-spaced lines in the centre of the diagram, the upper represents conformer E, and the lower, conformer C.

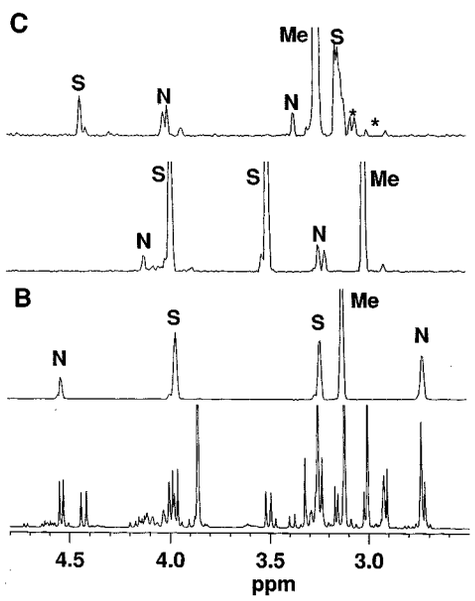

Fig. 4 Proton slices from the HMBC spectrum of DADS in dimethylformamide-d_7 at 253 K, together with the proton spectrum on the same scale. Conformer B, which is symmetrical, shows the diastereotopic protons of the N-CH_2 and the S-CH_2 groups, plus the *N*-methyl signal. In the asymmetric conformer, C, there are two carbonyl peaks in the ^{13}C spectrum. Each shows its corresponding N-CH_2, S-CH_2 and *N*-methyl signals. The variable intensities are due to poor digitization in the f_1 dimension. Signals marked with a star represent a small impurity.

of chemical shifts and coupling constants are given in the supplementary data.†

Molecular modelling, using the AM1 method in SPARTAN (version 5.0.3) and previous results,[1] gave a selection of candidate conformations for the molecule. This included both symmetrical *Z,Z* conformations (in the nomenclature used previously[1]) as well as the non-symmetric *Z,E*. The exact energies of the conformations, and their order, depended very much on the details of the modelling method used. Therefore, no quantitative information from the modelling has been used. However, the geometries fitted into six classes: the five shown in Fig. 1, and one *E,E*, which was not observed. The spectra were assigned to individual conformations using a phase-sensitive NOESY experiment (Fig. 6) at a temperature (253 K) at which chemical exchange is very slow. The vicinal couplings in the CH_2–CH_2 group (supplementary material)† were in the ranges of 11.2 to 13.0 Hz for the *trans* coupling, and either 3.0 to 5.0

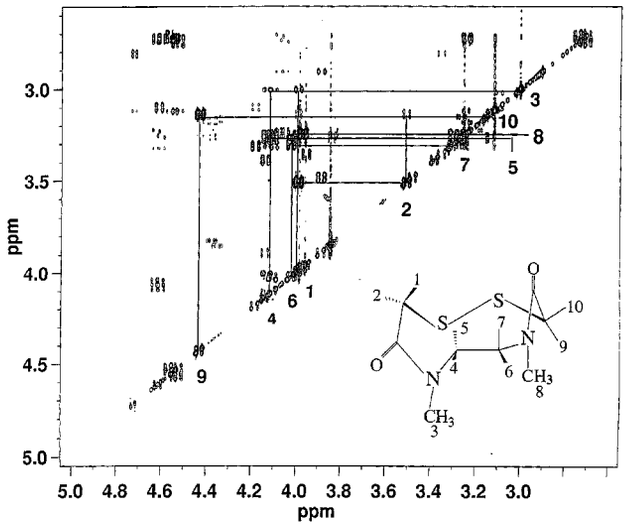

Fig. 5 Gradient COSY spectrum of DADS spectrum at 500 MHz, taken at 253 K—a temperature at which the chemical exchange is negligible. The correlations drawn in correspond to conformer C in Fig. 1.

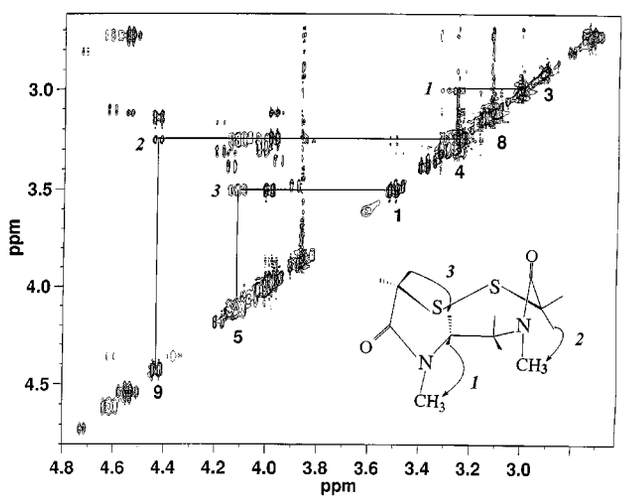

Fig. 6 500 MHz phase-sensitive NOESY spectrum of DADS at a temperature of 253 K. The labelling of the diagonal peaks corresponds to the structure in Fig. 5, and the lines correspond to the nOe's drawn on the structure.

Hz or 0 to 1.5 Hz for the two *gauche* couplings. These were not sufficiently different in different conformations to give useful geometrical information. In dimethylformamide solution, the lowest-energy conformer matches the *Z,E* conformation seen in the crystal structure.[1] For each species, the coordinates of each atom from the SPARTAN conformation are given in the supplementary material.†

The exchange mechanism was confirmed by doing a NOESY (EXSY) experiment at 275 K, when the processes with low barriers are in slow exchange. Fig. 7 shows a portion of the spectrum illustrating the exchange amongst conformations A, C and E in Fig. 1. Note that this spectrum was run with a long mixing time (0.8 s), so that cross peaks appear between C and E even though the final analysis shows little direct exchange.

Exchange rates were measured by one-dimensional methods. In the intermediate exchange region, lineshapes were simulated (Fig. 8) using the MEXICO program (available from Alex D. Bain[33]), and compared visually with the experimental spectra using the dual display features of the spectrometer software. Errors in these rate measurements are estimated at about 10%, so the error in $\Delta G^{\ddagger}$ is about $0.1RT$. Slower exchange rates were measured by doing selective-inversion experiments on the methyl signals.[34–37] Note that the selective-inversion experiments fit the whole of the exchange process, not just the initial

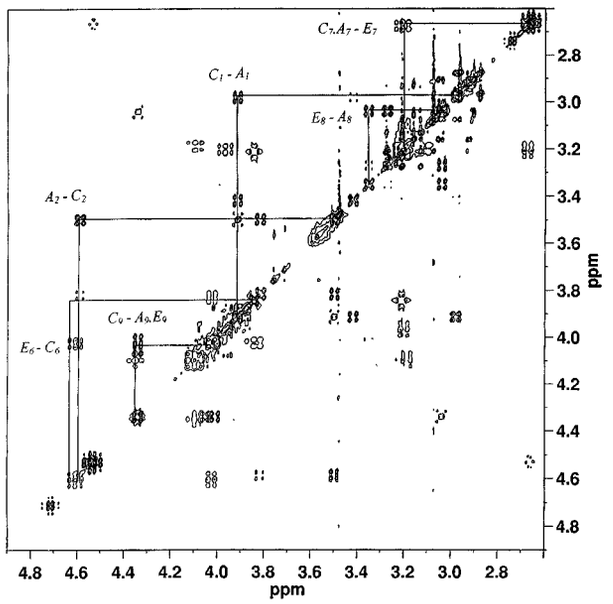

Fig. 7 500 MHz phase-sensitive EXSY spectrum of DADS taken at a temperature of 275 K. At this temperature, processes with the lower barriers (involving conformers A, C and E) are in slow, but observable, exchange. The spectra were taken with a long mixing time in order to map the whole exchange mechanism. The lines show the correlations for six of the protons in the molecule, numbered as in Fig. 5. The cross peaks between conformers C and E are second-order peaks, since little direct exchange could be measured between these two forms (see Fig. 9).

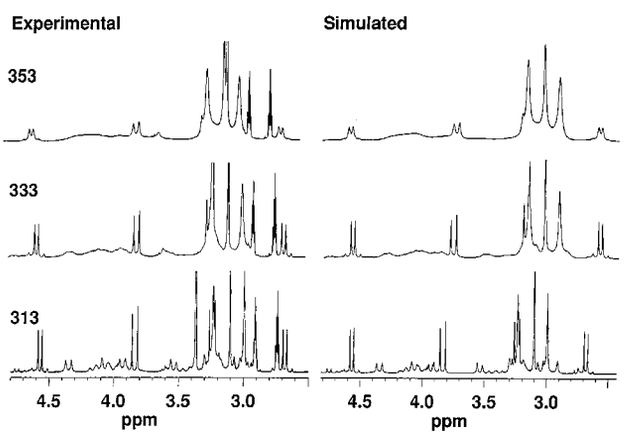

Fig. 8 Experimental (left) and simulated (right) 300 MHz proton NMR spectra of DADS at 313, 333 and 353 K. The spectra were simulated using the program MEXICO.

linear part. Fig. 9 illustrates this. If the magnetization of C is inverted, then E should show no change at time zero if there is no direct exchange between the two sites. In Fig. 9, the initial slope of the E magnetization is considerably smaller than that of A. At later times there is an indirect change, as was observed in the EXSY experiment in Fig. 7. The full observed relaxation, under the combined influence of spin-lattice relaxation and chemical exchange, was analyzed using the CIFIT program (available from Alex D. Bain).[38] Fig. 9 shows the quality of the fit of these data.

Discussion

The exchange rates are summarized in the Eyring plot in Fig. 10. The disulfide inversion and the ring flip process have the lowest barriers: $\Delta H^{\ddagger} = 72 \pm 1$ kJ mol^{-1} and $\Delta H^{\ddagger} = 74 \pm 1$ kJ mol^{-1}, respectively. The entropies of activation are close to zero: $\Delta S^{\ddagger} = 0$ within experimental error for the disulfide process and $\Delta S^{\ddagger} = 11 \pm 3$ J K^{-1} for the ring flip. The sizes of amide barriers[49] are typical: for the C to D process, $\Delta H^{\ddagger} = 86 \pm 1.5$ kJ

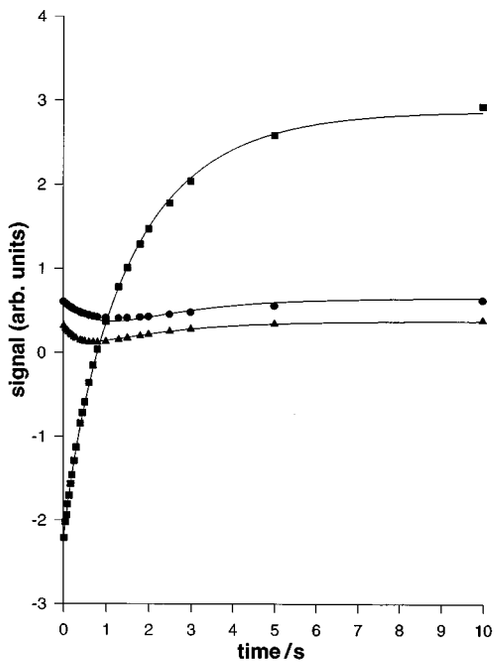

Fig. 9 Results of a selective-inversion experiment. One of the *N*-methyl signals of conformer C (represented by squares) was inverted. The triangles correspond to conformer A, and the circles to conformer E. The points represent measured values and the lines are the best fit to the data. Note the small slope at time zero of the signal E. This shows there is little direct exchange between conformers C and E.

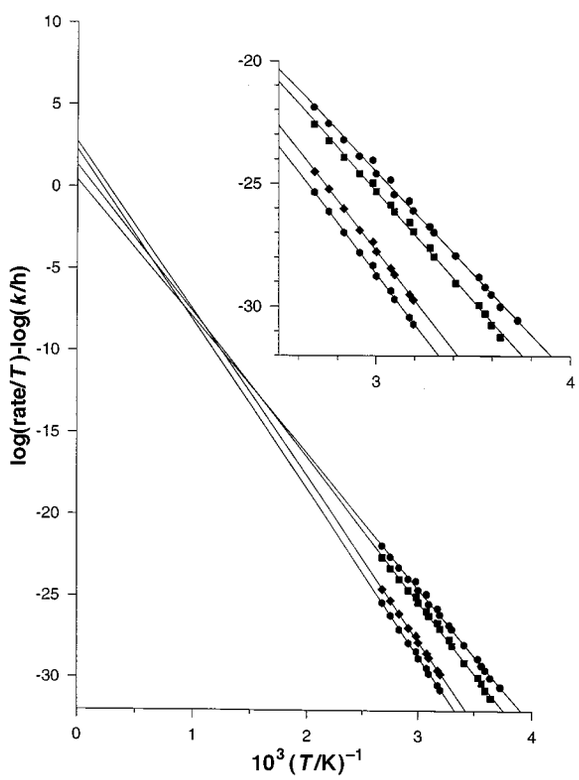

Fig. 10 Eyring plot of the rate data for the four observed exchange processes in DADS, plotted showing the *y* intercepts and expanded in the inset. The lowest set of experimental data (octagonal symbols) represent the C to D process, the next highest set (diamonds) represent A to B, the next set (squares) represent A to E, and finally the highest set (circles), the A to C process.

mol^{-1} and for the A to B process, $\Delta H^{\ddagger} = 84 \pm 1.2$ kJ mol^{-1}. However, both barriers have significant positive entropies of activation: $\Delta S^{\ddagger} = 19 \pm 4$ J K^{-1} and $\Delta S^{\ddagger} = 22 \pm 4$ J K^{-1}, respectively. This means that the barrier estimated from a single rate measurement and eqn. (1), $\Delta G^{\ddagger}$, would be different from a

calculated barrier, $\Delta H^{\ddagger}$, by approximately 6 kJ mol^{-1} at ambient temperature.

It appears that the disulfide can invert only if one of the amides is *E* - no firm evidence of direct interconversion of conformers B and D was observed. This seems to be a steric effect. The *Z*,*Z* form has a more crowded ring, since there is a methyl group and an amide oxygen on each side of the ring (Fig. 1). The modelling studies suggest that these groups are only 3.14 Å apart in conformer B, and 3.26 Å in conformer D. In the *Z*,*E* form (conformers C and A), there is only one amide oxygen on one side of the ring. Furthermore, the two methyl groups on the other side are 3.8–3.9 Å in both conformers. The distance from the methyl groups to the oxygen atom on the same side of the ring is even larger. This appears to give the ring sufficient flexibility so that conformer C can convert to conformer A without prohibitive steric hindrance.

Conclusions

This work is an example of how much detailed information is available through the application of modern one- and two-dimensional NMR methods. Measurement of the equilibrium constants and the exchange rates has provided nine experimental points on the potential energy surface. For the exchange rate determinations, a combination of slow and intermediate exchange techniques provides data over a wider temperature range. In particular, the one-dimensional selective-inversion experiments provide excellent rate data in the slow exchange regime. This means that the free energy of activation can be separated into enthalpy and entropy effects. The disulfide inversion and the ring flip process are dominated by enthalpy effects, but the two amide inversions show significant positive entropy contributions to the barriers. Fig. 1 summarizes the measured energies of the five local minima, and four of the transition states joining them. This system is by no means the limit of the methods used here, so systems that are larger and more complicated are still tractable.

Experimental

Preparation of DADS (Scheme 1)

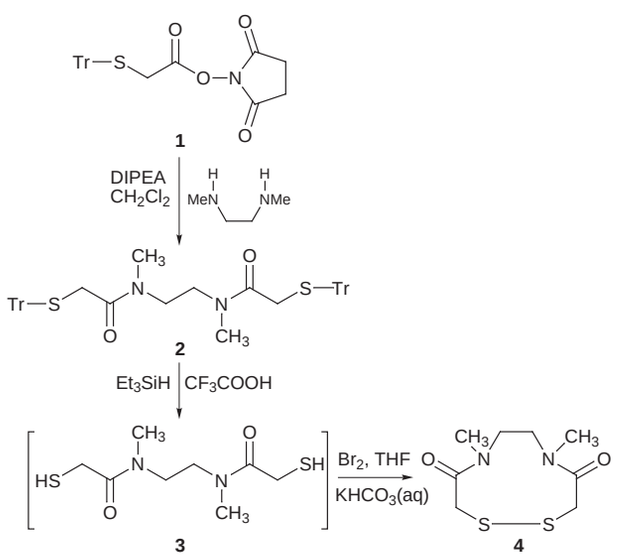

Scheme 1

Analytical TLC was performed on silica gel 60-F_{254} (Merck) plates, using a 10% v/v solution of methanol in dichloromethane as the eluent. Analysis of the plates was performed by irradiation with long wavelength ultraviolet light unless specified otherwise. All commercial reagents were used as supplied. All reactions were protected from light and carried out under a slow flow of nitrogen unless stated otherwise. Solvents were evaporated with a Buchi rotary evaporator (20 mmHg) at moderate temperatures (30–50 °C). Melting points were recorded on a Gallenkamp capillary tube melting point apparatus. Electron impact mass spectra were recorded on a VG Analytical ZAB-E double focusing mass spectrometer. Electrospray mass spectrometry (ES-MS) was performed with 50/50 CH_3CN–H_2O as the mobile phase at a flow rate of 1.5 mL per minute, with the use of a Brownlee Microgradient syringe pump. Solid samples were dissolved in 50/50 CH_3CN–H_2O immediately before analysis. Full scan ES-MS experiments were performed with a Fisons Platform quadrupole instrument. Compound **1** was synthesized following the procedure of Bell *et al.*[50]

Compound 2. To compound **1** (5.45 g, 12.6 mmol) in dichloromethane (50 mL), *N*,*N*′-dimethylethylenediamine (666 μL, 6.25 mmol) and freshly distilled diisopropylethylamine (2.1 mL) were added. The reaction was stirred at room temperature for 36 hours whereupon it was extracted with 0.05 M HCl (2 × 25 mL), 10% $NaHCO_3$ (2 × 25 mL) and distilled water (1 × 20 mL). The organic layer was dried over sodium sulfate and evaporated to dryness at reduced pressure. The resulting oil was dissolved in a minimum volume of acetone and cooled to 4 °C for 24 hours. The resulting precipitate was filtered, washed with cold water (50 mL) and dried under high vacuum. The product, a colourless solid (4.0 g, 89%) showed: mp 71–72.5 °C; ES-MS (positive): 766.3 ($M + 2Na^+$), 743.4 ($M + Na^+$), 721.2 ($M + H^+$), 243 (Tr^+).

Compound 4. To compound **2** (1.03 g, 1.43 mmol) in trifluoroacetic acid (10 mL), triethylsilane was added dropwise until the colour discharged. The resulting solution was stirred for 15 minutes and then filtered. The precipitate was washed with cold TFA (10 mL) and the filtrate subsequently evaporated *in vacuo*. Dichloromethane was added to the resulting oil and immediately evaporated (3 × 40 mL). After the yellow oil was dissolved in THF (1000 mL) and 10% $KHCO_3$ (100 mL), bromine was added (81 μL, 1.57 mmol) and the reaction stirred, protected from light for 48 hours. The THF was evaporated and the resulting aqueous solution extracted with dichloromethane (5 × 100 mL). The organic extracts were combined, dried over sodium sulfate and evaporated at reduced pressure. The resulting oil was dissolved in a minimum volume of THF and cooled to −10 °C for 48 hours. The resulting colourless precipitate was filtered and washed with cold THF. The product, a colourless solid (152 mg, 46%) showed: HRMS calculated for $C_8H_{14}N_2S_2O_2$ *m*/*z* 234.04930, found 234.049668.

NMR Spectroscopy

Approximately 30 mg of DADS was dissolved in dimethylformamide-d_7 (DMF-d_7, 99.5% D, ISOTEC), which had been dried over activated molecular sieves. The solution was filtered through glass wool upon transferring to a 5 mm medium walled NMR tube.

High resolution ^{1}H spectra were recorded at 253, 273 and 303 K at 500.13 MHz, using between 512 and 1024 scans for each spectrum. Spectral widths were typically 1300 Hz with 32 K data points. Most spectra were zero filled twice, and were apodized with a Gaussian broadening of between 0.3 and 0.5, and a Lorentzian broadening ranging between −1 and −2 Hz. All spectra were referenced to the central line of the low-frequency methyl pentet of DMF-d_7 at 2.74 ppm. A ^{13}C spectrum was obtained at 253 K at 125.76 MHz; 20000 scans were collected over a spectral range of 3125 Hz. The spectrum was referenced to the central line of the low-frequency septet of DMF-d_7 at 30.1 ppm.

All 2D experiments were performed on a Bruker DRX 500 spectrometer with a 5 mm inverse triple axis gradient probe. The proton and carbon 90° pulse widths were 6.6 and 11.60 μs,

respectively. All phase sensitive methods used time proportional phase incrementation. Most spectra were apodized with either sine or cosine bell. A high resolution HMBC spectrum optimized for long range couplings was obtained, using 100 scans per increment, with 256 increments, without carbon decoupling during acquisition. Linear prediction was employed in the carbon dimension to 512 data points using 100 coefficients. The spectral range was 3600 Hz in ^{1}H and 3125 Hz in ^{13}C.

A phase sensitive gradient NOESY spectrum was acquired at 253 K using a spectral width of 1300 Hz in both dimensions, 128 increments and 32 scans per increment. At a mixing time of 0.8 s no EXSY cross peaks were observed. The first proton dimension was linear predicted to 256 points using 50 coefficients, and was zero filled to 1 K, giving 1.3 Hz point^{-1} digital resolution.

A gradient COSY-45 was obtained at 253 K using most of the above mentioned parameters. Four scans were acquired for each of the 256 increments. The indirect proton was linear predicted to 512 points using 100 coefficients and was zero filled to 1 K, giving 1.2 Hz point^{-1}.

A series of COSY and NOESY spectra were recorded for 275, 295 and 303 K to measure the temperature dependence of the chemical shifts and to determine the exchange mechanism. For the COSY spectra 256 increments with 8 scans were acquired, over a spectral width of 1570 Hz. Each dimension has 1 K data points giving 1.5 Hz point^{-1} digital resolution. The phase sensitive gradient NOESY spectra were acquired under much the same conditions except that 512 increments were recorded with 16 scans each. In this case the first dimension was linear predicted up to 1 K data points using 50 coefficients and was zero filled to 2 K giving 0.8 Hz point^{-1}. Sine bell apodization was used in both dimensions.

A series of spectra were obtained at 300.13 MHz as a function of temperature for line shape analysis. The spectra were acquired with a Bruker AC 300 spectrometer using a 5 mm four-nucleus probe. Temperature control was maintained to within ±0.5 °C using a BVT 2000 temperature controller, and was monitored periodically by inserting a copper-constantan thermocouple in a 5 mm NMR tube into the probe. Temperatures ranged from 253 to 383 K where spectra were collected at 5 to 10 degree intervals. Between 512 and 2 K scans were recorded over a 4200 Hz spectral width. For each FID 32 K data points were collected giving 0.13 Hz point^{-1}.

Selective-inversion and inversion–recovery experiments were carried out at 500 MHz between 253 and 303 K to measure rates in the slow exchange regime. The selective inversion sequence used was a modification of the standard RD-180-VD-90-Acq sequence where a Gaussian shaped 180° pulse was used, tuned to the resonance of interest to be inverted. The variable delays (VD) for both experiments varied from 0.01 to 15 s, and the relaxation delays (RD) were typically 15 s. Experiments were performed on the *N*-methyl resonances of the C (*ca.* 3.01 and 3.26 ppm), A (*ca.* 3.02 and 3.16 ppm) and E (*ca.* 2.91 and 3.32 ppm) conformers and the *N*-methylene resonance of the B (*ca.* 5.53 ppm) conformer. In order to obtain rate measurements of both processes of the mechanism C↔A↔E processes inversion had to be carried out of C and E independently. Line intensity measurements were made with the XWINNMR software package. Along with data from the inversion recovery experiments, the selective inversion data were fitted to the differential equations reflecting the exchange and relaxation behaviour of this system using CIFIT. Inversions were carried out on the *N*-methylene resonances of B in order to see whether the B to D process was active.

Once an assignment was obtained of all five conformations and the exchange mechanism was determined a complete lineshape analysis was performed. This was done on an SGI Indy computer with MEXICO, a lineshape simulation program developed in this laboratory, which is capable of simulating at least a 5-spin system undergoing unequally populated exchange among up to 5 sites.

The rate measurements obtained from 253 to 363 K for all 4 processes, were plotted according to the Eyring equation giving values for both activation enthalpies and entropies. The standard deviation in the intercept was extrapolated to the *y*-axis including the contribution from the standard deviation in the slope.[51]

Acknowledgements

We would like to thank Dr Don Hughes for help with the NMR spectroscopy, and Dr Boris Zhorov for discussions about the molecular modelling. The Natural Sciences and Engineering Research Council of Canada provided financial support.

References

1 R. B. Maharajh, J. P. Synder, J. F. Britten and R. A. Bell, *Can. J. Chem.*, 1997, **75**, 140.
2 K. Schwochau, *Angew. Chem., Int. Ed. Engl.*, 1994, **33**, 2258.
3 D. Brenner, A. Davison, A. G. Jones and J. Lister-James, *Inorg. Chem.*, 1984, **23**, 3793.
4 D. Stepniak-Biniakiewicz, B. H. Chen and E. Deutsch, *J. Med. Chem.*, 1992, **35**, 274.
5 W. C. Klingensmith, A. R. Fritzberg, V. M. Spitzer, D. L. Johnson, C. C. Kuni, M. R. Williamson, G. Washer and R. Weil, *J. Nucl. Med.*, 1984, **25**, 42.
6 R. K. Hom and J. A. Katzenellenbogen, *Nucl. Med. Biol.*, 1997, **24**, 485.
7 A. Capretta, R. B. Maharajh and R. A. Bell, *Carbohydr. Res.*, 1995, **267**, 49.
8 D. Z. Avizonis, S. Farr-Jones, P. A. Kosen and V. J. Basus, *J. Am. Chem. Soc.*, 1996, **118**, 13031.
9 K. D. Kopple, K. K. Bhandary, G. Kartha, Y. S. Wang and K. N. Parameswaran, *J. Am. Chem. Soc.*, 1986, **108**, 4637.
10 K. D. Kopple, J. W. Bean, K. K. Bhandary, J. Briand, C. A. D'Ambrosio and C. E. Peishoff, *Biopolymers*, 1993, **33**, 1093.
11 M. J. Blackledge, R. Bruschweiler, C. Griesinger, J. M. Schmidt and R. R. Ernst, *Biochemistry*, 1993, **32**, 10960.
12 T. Shimizu, Y. Tanaka and K. Tsuda, *Int. J. Peptide Protein Res.*, 1983, **22**, 194.
13 K. A. Carpenter, P. W. Schiller, R. Schmidt and B. C. Wilkes, *Int. J. Peptide Protein Res.*, 1996, **48**, 102.
14 D. Kern, G. Kern, G. Scherer, G. Fischer and T. Drakenberg, *Biochemistry*, 1995, **34**, 13594.
15 E. Pinet, J. M. Neumann, I. Dahse, G. Girault and F. Andre, *Biopolymers*, 1995, **36**, 135.
16 J. H. Viles, J. B. Mitchell, S. L. Gough, P. M. Doyle, C. J. Harris, P. J. Sadler and J. M. Thornton, *Eur. J. Biochem.*, 1996, **242**, 352.
17 A. Lombardi, M. Saviano, F. Nastri, O. Maglio, M. Mazzeo, C. Isernia, L. Paolillo and V. Pavone, *Biopolymers*, 1996, **38**, 693.
18 W. E. Stewart and T. H. Siddall, *Chem. Rev.*, 1970, **70**, 517.
19 R. R. Fraser, G. Boussard, J. K. Saunders, J. B. Lambert and C. E. Mixan, *J. Am. Chem. Soc.*, 1971, **93**, 3822.
20 C. M. Deber, F. A. Bovey, J. E. Carver and E. R. Blout, *J. Am. Chem. Soc.*, 1970, **92**, 6191.
21 M. Ptak, *Biopolymers*, 1973, **12**, 1575.
22 K. W. Kim, F. Sugawara, S. Yoshida, N. Murofushi, N. Takahashi and R. W. Curtis, *Biosci. Biotechnol. Biochem.*, 1993, **57**, 787.
23 D. Jiao, M. Barfield, J. E. Combariza and V. J. Hrubny, *J. Am. Chem. Soc.*, 1992, **114**, 3639.
24 V. Renugopalakrishnan and R. Walter, *Z. Naturforsch., Teil A*, 1984, **39**, 495.
25 Z. Lidert, *Tetrahedron*, 1981, **37**, 967.
26 L. M. Jackman and F. A. Cotton, *Dynamic Nuclear Magnetic Resonance Spectroscopy*, Academic Press, New York, 1975.
27 F. A. L. Anet and A. J. R. Bourn, *J. Am. Chem. Soc.*, 1967, **89**, 760.
28 S. C. Cepas and M. North, *Tetrahedron*, 1997, **53**, 16859.
29 D. M. Pawar and E. A. Noe, *J. Am. Chem. Soc.*, 1996, **118**, 12821.
30 J. Sandstrom, *Dynamic NMR spectroscopy*, Academic Press, London, 1982.
31 G. Binsch, *J. Am. Chem. Soc.*, 1969, **91**, 1304.
32 D. A. Kleier and G. Binsch, *J. Magn. Reson.*, 1970, **3**, 146.
33 A. D. Bain and G. J. Duns, *Can. J. Chem.*, 1996, **74**, 819.
34 M. Grassi, B. E. Mann, B. T. Pickup and C. M. Spencer, *J. Magn. Reson.*, 1986, **69**, 92.
35 J. J. Led and H. Gesmar, *J. Magn. Reson.*, 1982, **49**, 444.

36 D. R. Muhandiram and R. E. D. McClung, *J. Magn. Reson.*, 1987, **71**, 187.
37 A. D. Bain and J. A. Cramer, *J. Magn. Reson.*, 1993, **103 A**, 217.
38 A. D. Bain and J. A. Cramer, *J. Magn. Reson.*, 1996, **118 A**, 21.
39 R. E. D. McClung and G. H. M. Aarts, *J. Magn. Reson.*, 1995, **115 A**, 145.
40 A. D. Bain, G. J. Duns, F. Rathgeb and J. Vanderkloet, *J. Phys. Chem.*, 1995, **99**, 17338.
41 M. Vasques, G. Nemethyl and H. A. Scheraga, *Chem. Rev.*, 1994, **94**, 2183.
42 J. Jeener, B. H. Meier, P. Bachmann and R. R. Ernst, *J. Chem. Phys.*, 1979, **71**, 4546.
43 C. L. Perrin and T. Dwyer, *Chem. Rev.*, 1990, **90**, 935.
44 K. G. Orrell, V. Sik and D. Stephenson, *Prog. Nucl. Magn. Reson. Spectrosc.*, 1990, **22**, 141.
45 C. L. Perrin and R. E. Engler, *J. Magn. Reson.*, 1990, **90**, 363.
46 C. L. Perrin and R. E. Engler, *J. Magn. Reson.*, 1996, **123 A**, 188.
47 R. E. Engler, E. R. Johnston and C. G. Wade, *J. Magn. Reson.*, 1988, **77**, 377.
48 S. F. Bellon, D. Chen and E. R. Johnston, *J. Magn. Reson.*, 1987, **73**, 168.
49 A. N. Taha, S. M. Neugebauer Crawford and N. S. True, *J. Am. Chem. Soc.*, 1998, **120**, 1934.
50 R. A. Bell, D. W. Hughes, C. J. L. Lock and J. F. Valliant, *Can. J. Chem.*, 1996, **74**, 1503.
51 A. D. Bain, G. J. Duns, S. Ternieden, J. Ma and N. H. Werstiuk, *J. Phys. Chem.*, 1994, **98**, 7458.

Paper 9/00502A